

One-Dimensional Cryogenic Temperature Measurement Using Rayleigh Scattering Thermometry with 266 nm Nd:YAG Laser

M. Seo¹, S. Jeong¹, J. Park² and H. Shin³

¹Cryogenic Engineering Laboratory, Department of Mechanical Engineering, KAIST, Daejeon, Republic of Korea

²HAE R&D Laboratory, LG Electronics, Seoul, Republic of Korea

³Combustion Engineering Laboratory, KAIST, Daejeon, Republic of Korea

ABSTRACT

Rayleigh scattering thermometry is an attractive technique to diagnose two-dimensional temperature distribution at cryogenic temperature due to no requirement for additional tracers or fluorescent particles in the visualization medium. Preliminary to the visualization of the temperature distribution in a pulse tube refrigerator, the validation experiment of laser Rayleigh scattering thermometry in 1-dimensional cryogenic temperature measurement is conducted and the results are discussed in this paper. In the experiment, the test cell of Rayleigh scattering thermometry is vacuum-insulated and is attached to a commercial Stirling cryocooler and electric heater to make the thermal equilibrium state from 230 to 295 K. We present the observation of the occurrence of the several stress-induced polarization phenomena in laser windows at the cryostat and the test cell and discuss its importance for Rayleigh scattering thermometry for low temperature.

INTRODUCTION

A pulse tube refrigerator (PTR) accommodates the working fluid under the condition of pulsating pressure and periodic oscillating flow to create the cooling effect. It is difficult to define the thermodynamic state and measure the specific working fluid properties in a pulse tube refrigerator unlike other steady stream refrigerators, such as J-T or reverse Brayton refrigerators. Also, many researches in regard to PTR depend on computational fluid dynamic (CFD) modeling and theoretical analysis because of its complex non-thermal equilibrium and the turbulent fluid characteristic within pulse tube components. The reasonable validation of high order CFD modeling of a PTR has not been achieved due to the lack of the detailed and precise measurements within pulse tube components¹. Additionally, for the development of large pulse tube refrigerator (LPTR) potentially useful for applied superconductor machines and industrial fields, it is getting important to identify and quantify the specific pulse tube losses.

For this reason, although the detailed measurement of temperature, pressure, and mass flow rate in a pulse tube component is needed, the complex fluid flow within a pulse tube component makes the measurement extremely difficult. Most of the experimental researches have, so far, measured the fluid properties locally to insert probe sensors at the inside or boundary of a pulse tube part²⁻⁵. These researches are limited to understand the complex thermal mechanism and the

losses comprehensively due to the limited measurements from a few sensors and locations. Also, these contact measurement methods can disturb the flow and temperature profiles of the fluid. Therefore, in the late 1990's, the visualization studies were initiated to overcome this measurement constraint in a pulse tube component. To investigate the flow pattern, velocity profile, and the secondary flow phenomena, experimental researches using a smoke-wire visualization technique were conducted⁶⁻¹⁰. Experiments using laser Rayleigh scattering thermometry to visualize the temperature profile in a pulse tube component were also carried out to calculate the enthalpy flow in order to understand the complex heat exchange phenomena^{11,12}. This laser-based approach is a pioneering application because it is the first attempt at the visualization technique of laser induced electromagnetic spectrum on the pulse tube visualization. The experimental set-up, however, was exposed to the room temperature and it was noted that it would be necessary to carry out a vacuum insulated experiment to investigate the pulse tube refrigerator accurately¹¹. Also, the calibration of the thermometry is conducted only at 270 K, though the Rayleigh scattering thermometry is applied from 350 K to 200 K in the main experiment¹³. The thorough calibration of Rayleigh scattering thermometry is necessary to achieve accurate measurements in a realistic PTR condition. For Rayleigh scattering thermometry at low temperatures, there are potential problems with respect to stress or pressure induced polarization effect in laser windows^{14,15}. For low temperature, the stress-induced polarization effect is unavoidable because the glass windows for visualization should be sealed with gaskets under mechanical stress. It is a serious problem because this polarization effect can change the composition ratio of linear polarization components and can create a retardance effect which makes elliptically polarized light from the linearly polarized light. Especially, the thermal stress-induced polarization effect occurring with temperature variation makes the calibration of thermometry fail. This polarization effect, however, is not considered at all in previous Rayleigh scattering thermometry researches.

In this paper, we present the experimental results and discussion of 1-D Rayleigh scattering thermometry in the modified experimental set-up at low temperature between 230 K to 295 K. It is observed how the thermal and mechanical stress-induced polarization phenomena occur in the sealed laser windows at the cryostat and the calibration test cell with vertically and horizontally polarized laser beam.

RAYLEIGH SCATTERING THERMOMETRY

Rayleigh scattering was originally used to measure the molecular density of gases, because the signal is linearly proportional to the number of scatterers, which means the gas molecules. Rayleigh scattering intensity, I_s , is expressed as follows¹⁶.

$$I_s = CIN\Omega l \left(\frac{d\sigma}{d\Omega} \right)_{\text{eff}} \quad (1)$$

where C is a calibration constant of the collection optics, I is the incident laser intensity, N is the molecular number density, Ω is the solid angle of the collection optics, σ is the Rayleigh scattering cross section area, l is the length of the laser beam segment imaged onto the detector. The molecular number density can be converted to the temperature using the ideal gas law.

$$I_s = CI\Omega l \frac{PA_o}{R_u T} \left(\frac{d\sigma}{d\Omega} \right)_{\text{eff}} = \frac{KP}{T} \left(\frac{d\sigma}{d\Omega} \right)_{\text{eff}} \quad (2)$$

where R_u is the universal gas constant, A_o is Avogadro's number, P is the gas pressure, and T is the gas temperature. Since all the optical values are assumed as constant, these optical constants and other ones, R_u and A_o , are converted to one representative constant, K . When the gas is pure, the differential Rayleigh scattering cross section area term can be assumed as constant as shown in Eq. (2). The constants are evaluated by temperature, pressure, and scattering intensity that are measured at the reference condition. Therefore, the temperature of the gas is described as follows¹¹.

$$T = \frac{I_{ref} P}{I_s P_{ref}} T_{ref} \quad (3)$$

Rayleigh scattering thermometry is a suitable method for low temperature measurement because this method does not need an additional tracer and the Rayleigh scattering intensity signal increases when the temperature decreases.

EXPERIMENTAL APPARATUS

As shown in Fig. 1(a), a 10 Hz pulsed Nd: YAG laser source (Continuum, Powerlite Precision II 8000) provides a horizontally polarized 266 nm laser beam. An ultraviolet 266 nm laser is appropriate for Rayleigh scattering thermometry, because the Rayleigh scattering cross section area is inversely proportional to the fourth power of the wavelength and the needless reflection light from the wall is reduced^{16,17}. When a half wave plate (HWP) is used, the polarization direction of laser is controlled. As shown in Fig. 1(b), the test cell is made of copper and is rectangular in shape. A black mat finish is applied inside the test cell to reduce the reflected background signal. The extended adaptor parts are installed at both sides of the laser inlet and outlet to further reduce the back reflection from the laser windows. The laser inlet, outlet, and the observation window of the test cell are 266 nm anti-reflection coated fused silica windows (Thorlab, high-precision laser window) with 1 inch diameter and 5 mm thickness. These windows are sealed with indium wire gasket for cryogenic sealing¹⁸. Five (5) E-type thermocouples are installed as a vertically cross-shaped form in the center of the test cell and two (2) silicon diode sensors are installed on the outside surface of the test cell to check the temperature difference between the test cell wall and the gas inside. Pressure in the test cell is measured from the pressure transducer (Honeywell, 1000 kPa, 0.1% acc.). The test cell is cooled by a commercial Stirling cryocooler (Cryotel CT, 4W cooling power @60 K). The degree of vacuum insulation is maintained under 1 mTorr during the experiment. The vacuum chamber also has the laser inlet, outlet, and the observation windows, and these windows are sealed with a rubber o-ring gasket and teflon. The laser inlet and the observation window are 79.5 mm diameter and 5 mm thickness quartz. The outlet laser window of the cryostat is 1 inch UV fused silica window and is installed on the adaptor with an inclined angle to prevent reflected laser beam from re-entering into the test cell. Additionally, to improve vacuum insulation and solve frost problem effectively, the copper panel coated with coconut charcoal which is a kind of moisture absorption material is installed around the test cell. Intensity of the Rayleigh scattering signal is measured by an ICCD camera (Princeton Instruments, PI-MAX2). We also measure laser beam power by photodiode (Thorlab DET25K, GaP detector) and boxcar averager (Stanford Research System, SR250 average) to compensate laser power fluctuation and drift.

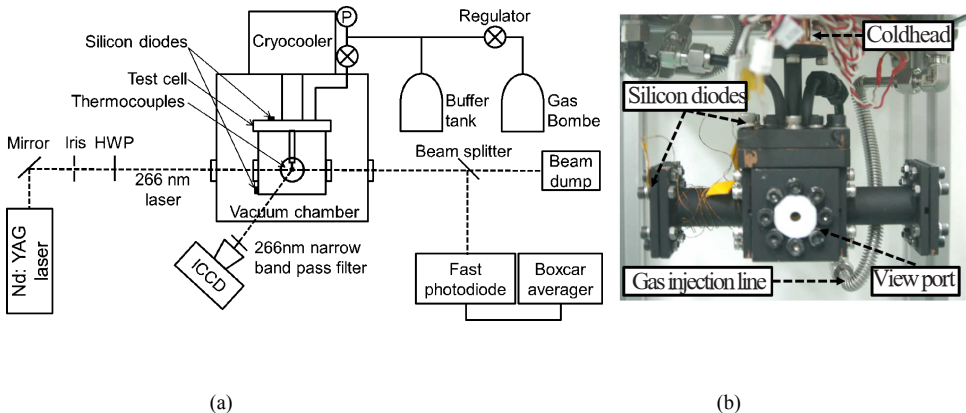


Figure 1. Experimental apparatus : (a) schematic diagram (b) photo of test cell

EXPERIMENTAL RESULTS AND DISCUSSION

Rayleigh scattering signal is dependent on the angle between a scattering measurement device and the direction of polarization of laser¹⁹. Since a scattering measurement device, such as an ICCD camera, is typically placed on the ground, a horizontally polarized laser provides a minimum scattering signal and a vertically polarized laser provides a maximum one. Therefore, by this characteristic, an indirect way to check the polarization direction is utilized in the experiment to take advantage of the measured scattering intensity from the ICCD camera instead of a polarization analyzer or a linear polarizer. When a linearly polarized laser beam passes through a half wave plate, the polarized direction of a laser beam is rotated symmetrically with the angle between the fast axis of a half wave plate and a polarized line of the laser beam as shown in Fig. 2(a). To confirm the validity of the method for checking the direction of the polarization of laser beam by measuring the scattering intensity, the preliminary test is conducted by changing the direction of polarization with rotation of a half wave plate and measuring the scattering intensity as shown in Fig. 2(b). The minimum scattering intensity and the laser power are obtained when the angle between the fast axis and the line of polarization is 0 and 90 degrees, because the direction of the laser beam polarization in this experiment is originally horizontal and is also horizontal after passing through a half wave plate. The maximum scattering intensity and the laser power are obtained when the vertically polarized laser beam is created from the horizontally polarized laser when the fast axis is placed on 45 degrees from a horizontal line. This result means that we can obtain the variation of polarized direction of the laser beam by measuring the scattering intensity from the ICCD camera.

The experiment is conducted to obtain the effect of mechanical stress to the laser window on the polarization features. Laser window is installed at the special adaptor which gives mechanical stress, the stress for vacuum sealing approximately, to a window and this device is placed between the iris and the laser inlet side of the vacuum chamber in Fig. 1(a). The polarization effect of the stressed laser window is obtained by rotating this adaptor with the laser window and simultaneously checking the scattering intensity. In Fig. 3(a), the scattering intensity is measured with the application of the horizontally polarized laser without a half wave plate. The scattering intensity of no stressed windows shows constant value, regardless of the rotation direction and angle of the laser window. This result means that there is no polarization effect of the stress-free laser window. It is the normal characteristic of the most frequently used optic devices, such as a normal fused silica window²⁰. Conversely, the stressed window tightened by screw bolts shows that the rotation of the laser window affects on the scattering intensity. This result indicates that

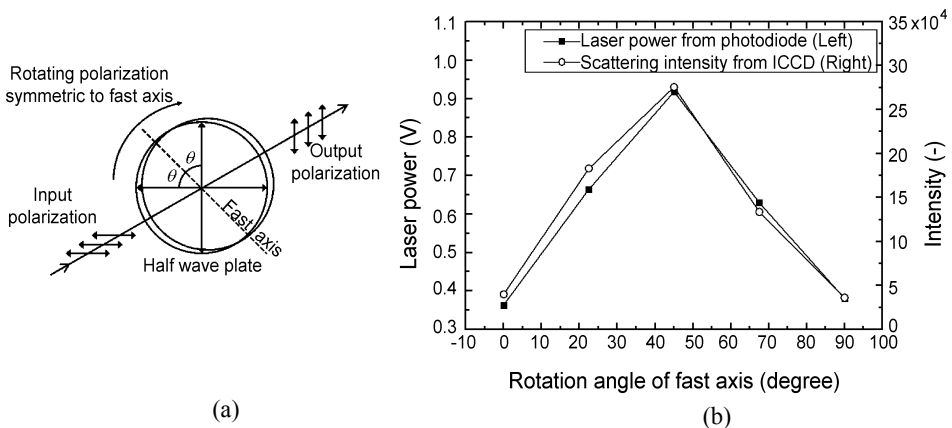


Figure 2. (a) A half wave plate mechanism (b) Laser power measured from photodiode and scattering intensity with the variation of the angle between the fast axis of the half wave plate and a horizontal line

the polarization effect occurs when the mechanical stress is applied on the laser window in contrast with the case of no-stressed window. The scattering intensity increases and the maximum intensity is 4 times its original value. Above mentioned, when the horizontally polarized laser is applied, the scattering intensity presents minimum value. Therefore, the intensity has to be increased by the polarization effect. As shown in Fig. 3(a), from the curves of the stressed window being rotated clockwise and counter-clockwise, it is obtained that the exact same curve is repeated and it means that the polarization effect evidently exists once the stress is applied and maintained. However, it gives different tendency when the laser is applied on the reversed window device. When the vertically polarized laser with a half wave plate is applied as shown in Fig. 3(b), the polarization effect by mechanical stress also does not occur in the case of no-stressed window and occurs in the case of strong-stressed window with the variation of rotation angle. This result means that the stress-induced polarization effect also occurs with vertically polarized laser by the mechanical stress. In contrast to Fig. 3(a), the scattering intensity of the stressed laser window is less than that of no stressed window because the maximum scattering intensity is supplied with the vertically polarized laser. When the vertically polarized laser is applied, the scattering intensity is already maximum. Therefore, the intensity cannot increase anymore that the original value. The ratio of scattering intensity change by the polarization effect with the vertically polarized laser is much smaller than the polarization effect with the horizontally polarized laser as shown in Fig. 3. Therefore, the vertical polarization of laser beam should be provided in Rayleigh scattering thermometry to achieve not only low sensitivity in regard to the polarization effect but also high scattering intensity signal. This polarization effect is caused by the stress-induced anisotropic phenomena in the glass material^{14, 20}. When the optically isotropic window, such as normal laser window, is changed to anisotropic material by stress, the window has birefringence and polarization characteristics, such as a polarizer or a wave plate. Therefore, the stress effect on polarization should be considered in the measurement of scattering intensity where cryogenic experiment is done with mechanically sealed window. Additionally, the other important point of this result is that this polarization effect occurs randomly and unregularly by the stress according to circumstance and fabricator. It means that it is very difficult to quantify this polarization effect. Therefore, in-situ examination of polarization effect is needed when Rayleigh scattering method is used for the closed or seal system.

For the calibration of Rayleigh scattering thermometry, the variation of Rayleigh scattering intensity as temperature is measured as shown in Fig. 4. Carbon dioxide is charged at 800 kPa instead of nitrogen to achieve high scattering signal due to its high Rayleigh scattering cross

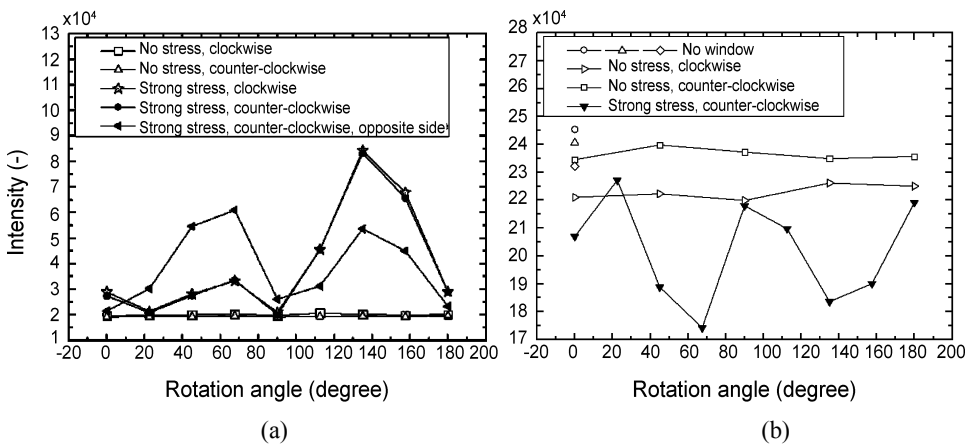


Figure 3. Scattering intensity variation with the rotation angle of laser window in the condition under no stress and strong mechanical stress applied with (a) horizontally and (b) vertically polarized laser beams

section area. The predicted line displayed in Fig. 4 is the normalized variation of molecular number density from ideal gas equation at constant pressure. Since the reference condition is selected as the highest temperature near room temperature, the predicted and measured curve starts concurrently at the reference point. As shown in Fig. 4(a), the scattering intensity with horizontally polarized laser has significantly larger value than the predicted line at low temperature. Conversely, in Fig. 4(b), the tendency of scattering intensity curve with vertically polarized laser is different from the curve of Fig. 4(a). The better agreement is achieved, but the measurement curve also becomes inaccurate as temperature decreases and presents less value than the predicted line at 230 K. Before this experiment, the validation of experimental set-up for measuring the molecular number density of gas is confirmed by checking linearity with varying pressure at constant temperature condition. However, the measured scattering intensity in Fig. 4 which means the molecular number density is seriously disagreed with the predicted curve. All variables in Eq. (1) are controlled in this experiment. The only variable which is not included in Eq. (1) is the polarization effect. Besides, there is significantly different disagreement tendency depending on the polarized type of applied laser, whether it is horizontal or vertical polarization as shown in Fig. 4.

Figure 5 shows the measured laser power from the photodiode with various temperature conditions. After the laser beam is passed through the test cell and the vacuum chamber, a part of laser beam is reflected at the beamsplitter and enters to the photodiode as shown in Fig. 1(a). The beamsplitter has the different reflectance in regard to horizontal and vertical polarization laser beam, respectively. Therefore, as shown in Fig. 5, the significant variation of photodiode signal in the conditions of temperature variation means that the polarization component of laser beam is changed in contrast to minor change of photodiode signal at constant temperature conditions.

Accordingly, by all these reasons, the significant disagreement in Fig. 4 is caused by the polarization effect with temperature change. As it is mentioned in the introduction section, thermal stress which is induced by different thermal expansion coefficients of the assembled materials results in the polarization effect. Therefore, this polarization effect can be called thermal stress-induced polarization effect. Fig. 4(a) can be explained that the scattering intensity increases because the vertically polarized component in the laser beam is created from the horizontally polarized laser beam as temperature decreases. Also, Fig. 4(b) is explained by the

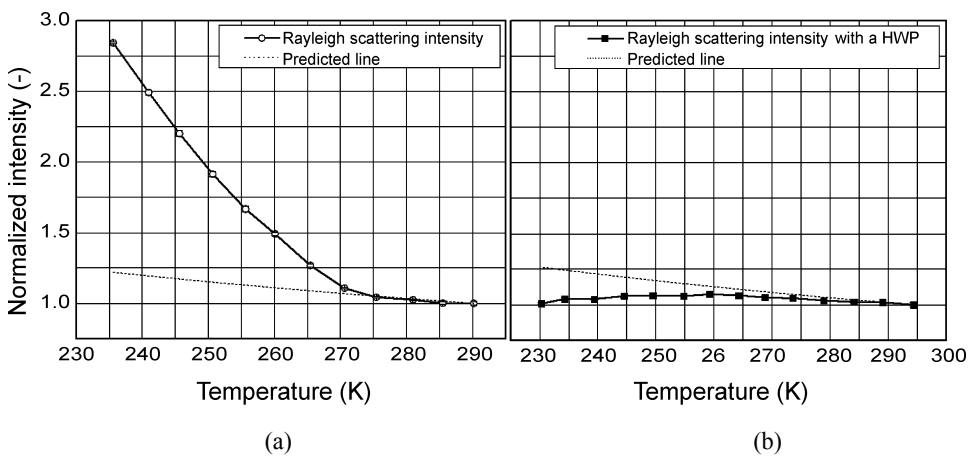


Figure 4. Normalized scattering intensity with temperature variation of (a) horizontally and (b) vertically polarized laser beam at constant pressure condition

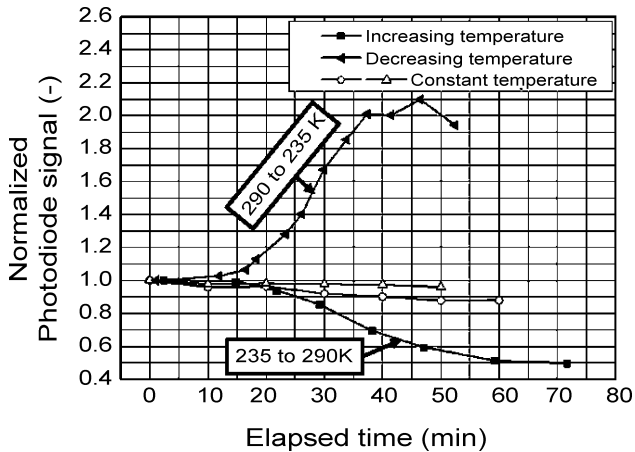


Figure 5. Normalized photodiode signal of various temperature conditions as time elapses

opposite situation. The analysis of thermal stress-induced polarization effect is very complex because it is dependent on the condition of thermal transient situation, the degree of thermal insulation, and environmental temperature. Therefore, for the experiment including a window-sealed part, such as cryogenic visualization experiment, the experimental set-up should be designed with thermal stress-free window or glass.

In this paper, we suggest some solutions to reduce the thermal and mechanical stress-induced polarization on the laser window in a cryogenic experiment. These solutions are not verified, but it is clear that these methods have more positive effects qualitatively than the existing methods to reduce the stress-induced effect. First of all, there was previous research in the stress-free window for laser application with the plurality of circular and curved grooves on the window surface to prevent stresses from reaching the central region of the window used for light beam transmission¹⁴. Although the fabrication of the grooved glass window is difficult, it would be the most effective way to reduce stress effect, if possible. Second, in a similar way, the larger diameter window is applied, the less stress in the center of a window, because the stress at the boundary of window also cannot reach the center of a window as the window size becomes large. Not only for 1-D calibration but also for 2-D visualization, a double ended glass (quartz) to metal (stainless steel 304) tubular adaptor is recommended because it is not needed to apply additional mechanical stress to seal a quartz glass. Besides, when designing quartz-to-metal seals, the intermediate material is commonly added between quartz and metal to reduce thermal stress effect due to the difference of the thermal expansion coefficient.

CONCLUSION

We conduct the experiment to calibrate 1-D Rayleigh scattering thermometry for low temperature measurement applying 266 nm laser. It is obtained that the thermal stress-induced polarization effect at a laser window which is not considered in the past researches should be corrected in the experiment at low temperature including window-sealed components. For accurate Rayleigh scattering thermometry, it is recommended that the thermally and mechanically stress-free components are to be utilized and in-situ calibration process is to be performed.

ACKNOWLEDGMENT

This research was supported by the Converging Research Center Program funded by the Ministry of Education, Science and Technology (No. 2011K00078).

REFERENCES

1. Taylor, R. P., "Development and Experimental Validation of a Pulse Tube Design Tool Using Computational Fluid Dynamics," Doctor of Philosophy Dissertation, *The University of Wisconsin-Madison*, (2009).
2. Rawlins, W., Radebaugh, R., and Timmerhaus, K. D., "Thermal anemometry for mass flow measurement in oscillating cryogenic gas flows," *Review of Scientific Instruments*, Vol. 64, Issue: 11 (1993), pp. 3229-3235.
3. Tanaka, M., Kawamatsu, S., Kodama, T., Nishitani, T., Kawaguchi, E., and Yanai, M., "Behavior of the gas temperature and pressure in the pulse tube refrigerator," *Cryogenics*, Vol. 32, Supplement 1, (1992), pp. 32-35.
4. Seo, K., Shiraishi, M., Nakamura, N., and Murakami, M., "Investigation of Radial Temperature and Velocity Profiles in Oscillating Flows Inside a Pulse Tube Refrigerator," *Cryocoolers 9*, Plenum Press, New York (1997), pp. 365-374.
5. Jeong, S., Nam, K., Kim, M., Chang, H., and Jeong, E., "Experimental Study of the Heat Transfer in Pulse Tubes," *Cryocoolers 11*, Kluwer Academic/Plenum Publishers, New York (2001), pp. 345-351.
6. Lee, J. M., Kittel, P., Timmerhaus, K. D., and Radebaugh, R., "Flow Patterns Intrinsic to the Pulse Tube Refrigerator *7th International Cryocooler Conference Proceedings*, Air Force Phillips Laboratory Report PL-CP--93-1001, Kirtland Air Force Base, NM, April 1993, pp. 125-139.
7. Shiraishi, M., Nakamura, N., Seo, K., and Murakami, M., "Visualization study of velocity profiles and displacements of Working Gas Inside a Pulse Tube Refrigerator in the 9th International Cryocooler Conference," *Cryocoolers 9*, Plenum Press, New York (1997), pp. 355-364.
8. Shiraishi, M., Takamatsu, K., Murakami, M., Nakano, A., Iida, T., and Hozumi, Y., "Visualization of DC Gas Flows in a Double-Inlet Pulse Tube Refrigerator with a Second Orifice Valve in 11th International Cryocooler Conference," *Cryocoolers 11*, Kluwer Academic/Plenum Publishers, New York (2001), pp. 371-379.
9. Shiraishi, M., Takamatsu, K., Murakami, M., and Nakano, A., "Dependence of Convective Secondary Flow on Inclination Angle in an Inclined Pulse Tube Refrigerator Revealed by Visualization," *Cryogenics*, Vol. 44, Issue: 2 (February 2004), pp. 101-107.
10. Shiraishi, M., Murakami, M., and Nakano, A., "Visualization of Secondary Flow in Tapered Double-Inlet Pulse Tube Refrigerators," *Cryocoolers 13*, Kluwer Academic/Plenum Publishers, New York (2005), pp. 313-322.
11. Hagiwara, Y., Nara, K., Ito, S., and Saito, T., "Temperature measurement in pulse tube with Rayleigh scattering and computation of enthalpy flow," *Cryogenics*, Vol. 39, Issue: 5 (May 1999), pp. 425-434.
12. Nara, K., Hagiwara, Y., and Ito, S., "Measurements of Gas Temperature in a Pulse Tube Using the Planar Laser Rayleigh Scattering Method in 10th International Cryocooler Conference," *Cryocoolers 10*, Plenum Publishing Corp., New York (1999), pp. 395-403.
13. Ito, S., Hagiwara, Y., Nara, K., "Study of Temperature Measurement in a Pulse Tube with Rayleigh Scattering," *Journal of The Cryogenic Society of Japan*, Vol. 33, No. 4 (1998), pp. 225-232.
14. Podgorski, T.J., "Stress-Free Window For Laser Applications," US Patent Vol. 4,421,386, Honeywell Inc., (December 20, 1983)
15. Sparks, M., and Cottis, M., "Pressure induced optical distortion in laser windows," *Journal of Applied Physics*, Vol. 44, Issue: 2 (1973), pp. 787-794.
16. Dibble, R. W., and Hollenbach, R. E., "Laser Rayleigh thermometry in turbulent flames," *Symposium (International) on Combustion*, Vol. 18, No. 1 (1981), pp. 1489-1499.
17. Koch, A., Voges, H., Andresen, P., Schlüter, H., Wolff, D., Hentschel, W., Oppermann, W., and Rothe, E., "Planar imaging of a laboratory flame and of internal combustion in an automobile engine using UV Rayleigh and fluorescence light," *Applied Physics B: Lasers and Optics*, Vol. 56, No. 3 (1993), pp. 177-184.
18. Miura, Y., "An optical window with thermal contraction free seal for low temperature use," *Cryogenics*, Vol. 22, Issue: 7 (July 1982), pp. 374-375.